

# Coherent optical phase transfer over a 32-km fiber with 1-s instability at $10^{-17}$

Seth M. Foreman<sup>1</sup>, Andrew D. Ludlow<sup>1</sup>, Marcio H. G. de Miranda<sup>1</sup>,

Jason E. Stalnaker<sup>2</sup>, Scott A. Diddams<sup>2</sup>, and Jun Ye<sup>1</sup>

<sup>1</sup>*JILA, National Institute of Standards and Technology and University of Colorado*

*Department of Physics, University of Colorado, Boulder, CO 80309-0440 and*

<sup>2</sup>*Time and Frequency Division, MS 847, National Institute of Standards and Technology, Boulder, Colorado 80305, USA*

(Dated: February 5, 2018)

The phase coherence of an ultrastable optical frequency reference is fully maintained over actively stabilized fiber networks of lengths exceeding 30 km. For a 7-km link installed in an urban environment, the transfer instability is  $6 \times 10^{-18}$  at 1-s. The excess phase noise of 0.15 rad, integrated from 8 mHz to 25 MHz, yields a total timing jitter of 0.085 fs. A 32-km link achieves similar performance. Using frequency combs at each end of the coherent-transfer fiber link, a heterodyne beat between two independent ultrastable lasers, separated by 3.5 km and 163 THz, achieves a 1-Hz linewidth.

Optical atomic clocks with superior stability and accuracy [1, 2] demand frequency transfer networks of unprecedented stability for signal distribution, remote synchronization and intercomparison. Clock signal transfer via optical fiber networks has emerged as a promising solution [3] when phase noise in the long transmission path has been effectively cancelled [4, 5, 6]. In the microwave domain, signals in the form of amplitude modulation of an optical carrier have been transmitted over an 86-km optical fiber network, where active stabilization of the fiber's group delay allows a transfer instability of  $5 \times 10^{-15}$  at 1-s and  $2 \times 10^{-18}$  after 1 day [7]. However, a direct transfer of the optical carrier itself [8, 9] is destined to achieve better stability, relying on the same advantage of high spectral resolution as the optical clocks. Long-distance coherent transfer of an ultrastable optical carrier signal, along with frequency-comb-based optical coherence distribution across the entire visible spectrum [10, 11], permits a wide variety of applications. They include phase-coherent large arrays of radio telescopes [12], precisely synchronized advanced light sources based on large-scale accelerators [13, 14], and precision optical interferometry over a long distance or encircling a large area.

In this Letter, we report experimental implementations of a fully coherent ( $< 1$  rad of accumulated optical phase noise) optical-frequency-distribution fiber system spanning tens of kilometers in distance and hundreds of nanometers in optical spectrum. While 1-s instability of  $6 \times 10^{-17}$  has been achieved in shorter ( $< 1$ -km) links [11], the  $2 \times 10^{-17}$  instability achieved here on a  $> 10$ -km link is  $\sim 2$  orders of magnitude lower than previously published results [9, 12]. In a 7-km fiber network installed in an urban environment, the transmission instability is reduced to  $6 \times 10^{-18}$  at 1 s and  $1 \times 10^{-19}$  at  $10^5$  s, limited by the out-of-loop measurement scheme. The accumulated phase noise, integrated from 8 mHz to 25 MHz, is 0.15 rad, representing a coherent optical transfer for timescales substantially longer than the coherence times of the current best optical references. An extended 32-km link employs a transceiver configuration, which is an im-

portant first step towards the realization of coherent repeaters for unlimited distribution distances. The system achieves similar stability performance. Using frequency combs at each end of a third fiber link, we remotely compare two Hz-linewidth lasers separated by 3.5 km of fiber and spectrally separated by 163 THz. The effective heterodyne optical beat has a 1-Hz linewidth, limited by the ultrastable lasers.

Figure 1 shows the experimental scheme for phase-coherent optical carrier transfer. To eventually compare the  $^{87}\text{Sr}$  optical lattice clock [2] at JILA to other optical clocks located at NIST [1, 15], we transmit the light from a cw 1064-nm laser, which can be directly measured with Ti:sapphire-based frequency combs serving as the optical clockwork at both locations. For active cancellation of the fiber network's phase noise, the transfer laser's coherence time must be longer than  $T_{rt}$ , the fiber network's round-trip time. The transfer laser used here has an intrinsic linewidth of 1 kHz in 1 ms, sufficient for fiber noise cancellation over the 7-km link. For longer fiber links and the remote ultrastable laser comparison, the transfer laser must be stabilized to a sub-Hz linewidth 698-nm laser [16] serving as the  $^{87}\text{Sr}$  clock's local oscillator. A self-referenced, octave-spanning Ti:sapphire laser is used to transfer the clock laser's phase-stability across the 148-THz spectral gap to the transfer laser.

For the fiber noise cancellation,  $\sim 1$ -mW from the transfer laser is picked off by a polarizing beamsplitter (PBS) and detected on photodiode PD1, while  $\sim 40$  mW is coupled into the fiber (below threshold for stimulated Brillouin scattering) after being frequency-shifted by an acousto-optic-modulator (AOM). Light returning from the fiber network's remote end accumulates a round-trip phase, again passes through the AOM, and is heterodyned with the local light on PD1. The beat frequency  $f_{\text{inc}}$  is used for fiber noise cancellation by phase-locking it to a radio-frequency (rf) reference via active feedback to the AOM's driving frequency [5, 6]. Noise processes that are stationary during  $T_{rt}$  (noise bandwidth  $< 1/2\pi T_{rt}$ ) are therefore pre-compensated by the AOM, whereas noise at frequencies above this bandwidth is un-

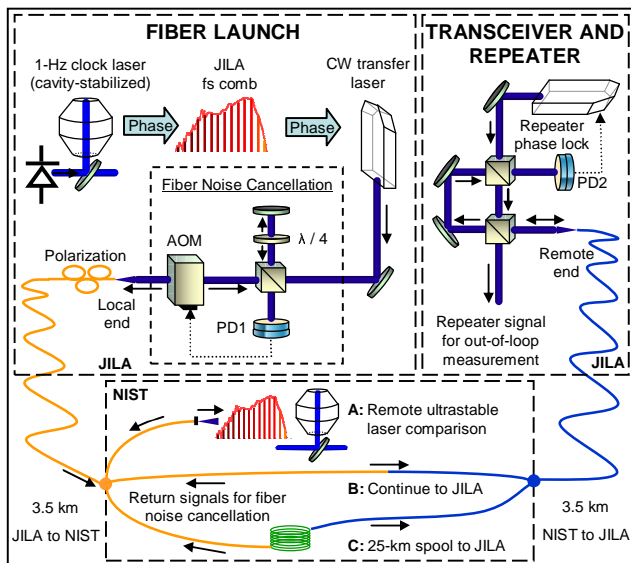


FIG. 1: (color online) Schematic for phase-coherent transfer of an optical carrier. At the Fiber Launch the cw transfer laser can be stabilized to a sub-Hz-linewidth clock laser via a fs frequency comb, or left free-running. The Fiber Noise Cancellation uses a double-pass AOM as the actuator. Round-trip light used in-loop for the noise cancellation comes from either a transceiver/repeater laser (transceiver method), or from a partially reflective gold coating on the flat tip of the fiber (reflection method), at the remote end of the network. Fiber networks of three different lengths are characterized.

cancelled. Due to burst noise in the fiber link, digital pre-scaling of  $f_{\text{fnc}}$  by a division of 50 is used to give the phase lock enough dynamic range to avoid cycle slips.

We test two methods for returning light from the fiber's remote end for noise cancellation. The simpler technique (reflection method) relies on partially reflective gold coating applied to the flat-polished remote fiber tip. The gold film transmits  $\sim 10\%$  of the incident 1064-nm light, and reflects the rest back to the launch port. The transmitted light is used for out-of-loop measurements of the stabilized fiber network. A more complex technique (transceiver method) uses an angle-polished remote fiber tip and an independent cw laser (transceiver laser) operating at the remote end. Light transmitted one-way through the fiber network is heterodyned with the transceiver laser on PD2, and the resulting beat signal is used to phase lock the transceiver laser to the transmitted light with a controllable constant frequency offset. Then  $\sim 40$  mW of light from the transceiver laser is launched into the fiber network's remote end, to be used for the in-loop fiber noise cancellation at the launching end. Additional power from the transceiver laser is used as a repeater signal for out-of-loop measurements of the stabilized fiber network. The reflection method is simple but can be corrupted by unwanted reflections at interconnections along the fiber network. The more-complex

transceiver method avoids this problem since a different frequency is returned than the input frequency. Also, the transceiver method boosts the power at the remote end and already realizes the setup necessary for a repeater station in a much longer fiber network.

Polarization considerations for both methods are essential. A set of fiber polarization paddles is used on the input end of the fiber link to adjust the polarization of the round-trip light to maximize the power of  $f_{\text{fnc}}$ . The power still fluctuates by  $\sim 1$  dB at frequencies of a few Hz, and slowly degrades by as much as 5 to 10 dB over the course of one day due to time-changing birefringence of the fiber network. Every few hours the polarization paddles are adjusted to maximize the strength of  $f_{\text{fnc}}$ . Another concern is fast time-changing polarization mode dispersion [17]. For the transceiver method it is necessary to ensure that the polarization used to stabilize the transceiver laser is the same as that it returns through the fiber network, so linear polarizers are placed immediately outside both ends of the fiber. Without the polarizers the fiber noise cancellation can not even be locked, but with them it can be maintained indefinitely with even less sensitivity to the fiber's changing birefringence than the reflection scheme. Rotating the polarization paddles to degrade the power in  $f_{\text{fnc}}$  by as much as 10 dB does not affect the quality of the lock.

The bottom panel of Fig. 1 shows how the fiber network can be configured in three lengths for various measurements. Two 3.5-km fibers in the Boulder Research and Administrative Network (BRAN) connect JILA with NIST [8]. In setup A, only one noise-cancelled fiber (reflection method) is used to transmit light for comparing the clock laser at JILA to an independent ultrastable laser at NIST [18] serving as the  $\text{Hg}^+$  clock laser. A second octave-spanning frequency comb at NIST [19] spans the 15-THz spectral gap between the transfer laser and the 1126-nm clock laser. A heterodyne beat between the transfer laser and one mode of the frequency comb at NIST is used as the effective beat between the two remotely-located clock lasers. In setup B, the two 3.5-km fibers are connected together to form a single 7-km (one-way) fiber network. The 7-km fiber has the local and remote ends located on the same table, allowing direct out-of-loop measurement of the transfer system when operated with either the reflection method or the transceiver method. In setup C, a 25-km spool of SMF-28 fiber is added to the 7-km link. With the additional loss of the spool (factor of 500 at 1064-nm each way) the reflection method is no longer practical, and only the transceiver method is characterized for the 32-km link. No special care is taken to isolate the spool from its environment. For all three setups, the first and last 5-m sections of fiber are single-mode for 1064-nm light in an effort to mitigate any effects of time-changing transverse mode dispersion from the slightly multi-mode BRAN fiber. Attenuation through 7 km of the fiber at 1064 nm is measured to

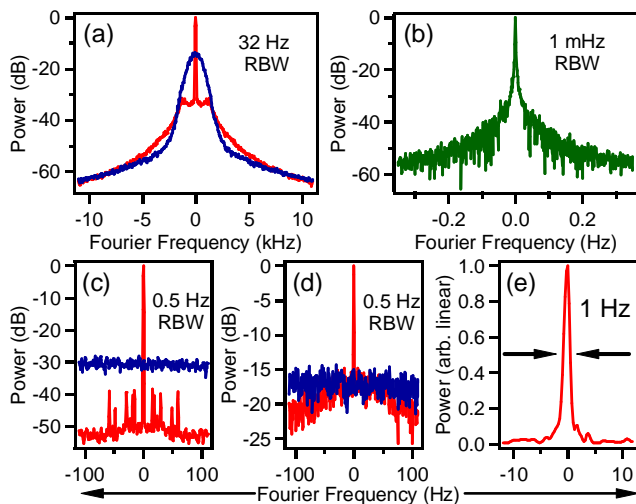


FIG. 2: (color online) Power spectra of various out-of-loop heterodyne beats. (a)  $f_{\text{tfr,tfr}}^{(7)}$  characterizes the 7-km transfer only (b)  $f_{\text{fs,tfr}}^{(7)}$  additionally characterizes the transfer laser's lock to the local fs comb. (c) same as (a), at finer resolution. (d)  $f_{\text{fs,rpt}}^{(32)}$  characterizes the 32-km transfer as well as the transfer laser's lock to the local fs comb. (e)  $f_{698,1126}$  is the effective beat between independent clock lasers separated by 3.5 km and 163 THz. For (a), (c), and (d) red is for the actively-stabilized network and blue is for the passive case.

be  $< 4$  dB. All but one interconnection along the 7-km fiber path is fusion spliced to reduce unwanted reflections, leading to the improvement over previous results [8].

The out-of-loop measurements are made using several different heterodyne beats. We adopt a notation in writing the beat frequencies as  $f_{\text{loc,rem}}^{(\text{dist.})}$ , where the first and second subscripts describe light at the local and remote ends, respectively. The superscript denotes the length (km) of the stabilized fiber link. Explicitly, the beat between the local transfer laser and the remote light exiting the gold-coated fiber is written as  $f_{\text{tfr,tfr}}^{(7)}$ , and  $f_{\text{tfr,rpt}}^{(7)}$  denotes the beat between the local transfer laser and the repeater light from the remote transceiver laser. Similarly, the beat between a mode of the local frequency comb and the remote light exiting the gold-coated fiber is  $f_{\text{fs,tfr}}^{(7)}$  while  $f_{\text{fs,rpt}}^{(7)}$  denotes the local comb's beat frequency against the remote repeater's light for the 7-km link. For the 32-km link, only  $f_{\text{fs,rpt}}^{(32)}$  is characterized. Measurements against the local transfer laser give information only about the fiber link, whereas measurements against the local frequency comb include the phase lock between the transfer laser and frequency comb.

Figure 2 summarizes the results of linewidth characterization for the various measurements. Figure 2(a) displays the power spectrum of  $f_{\text{tfr,tfr}}^{(7)}$  to characterize the 7-km fiber transfer. The uncancelled fiber noise broadens the transferred linewidth to  $\sim 1$  kHz, while the coherent narrow peak is achieved under active fiber noise cancel-

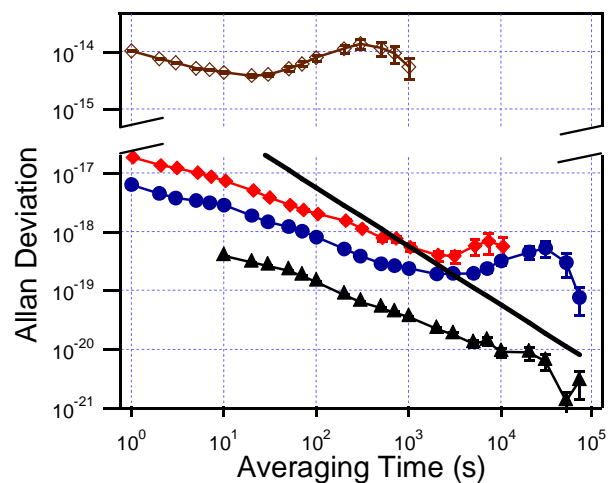


FIG. 3: (color online) Instability of the transfer systems. Open brown diamonds are typical passive instabilities of the 7- and 32-km fiber links. Closed red diamonds are for the 32-km system, measured by frequency counting  $f_{\text{fs,rpt}}^{(32)}$ . Closed blue circles are for the 7-km fiber transfer, using  $f_{\text{tfr,tfr}}^{(7)}$ . Black triangles are the instability of  $f_{\text{inc}}$  used for in-loop noise cancellation. The solid black line represents 1 radian of accumulated phase noise during the averaging time.

lation, with a 1.3-kHz servo bandwidth limited by  $T_{rt}$  for the 14-km round trip. Figure 2(c) shows the same data at finer resolution; the energy that spread into a 1-kHz bandwidth by the passive fiber's phase noise is replaced into the narrow central carrier under active noise cancellation. Figure 2(b) shows  $f_{\text{fs,tfr}}^{(7)}$  as a way to additionally characterize the transfer laser's lock to the local frequency comb; the full system operates with a sufficiently small phase noise that a 1-mHz linewidth is recovered. Figure 2(d) shows  $f_{\text{fs,rpt}}^{(32)}$  with active noise cancellation of the 32-km link (narrow carrier in red) and without noise cancellation (flat noise in blue). A narrow coherent feature is present at 0.5-Hz resolution bandwidth, but with less signal-to-noise than for the 7-km transfer because the servo bandwidth is smaller for the longer link. Finally, Fig. 2(e) shows the effective heterodyne beat between the two stable clock lasers at JILA and NIST, linked by the 3.5-km noise-cancelled fiber and two independent optical combs. The whole system preserves the full phase coherence of our optical frequency references.

We also directly count the frequencies of the various out-of-loop heterodyne beats. For improved counting resolution, we mix the beat frequencies to 10 kHz using a sufficiently stable rf source. Figure 3 displays the resultant Allan deviations. The open diamonds (in brown) show a typical passive instability for both the 7- and 32-km links. Closed diamonds (in red) are from counting  $f_{\text{fs,rpt}}^{(32)}$  to measure the instability of the 32-km transceiver system. Closed circles (in blue) use  $f_{\text{tfr,tfr}}^{(7)}$  to measure the instability of the 7-km fiber transfer (reflection method).

Closed triangles (in black) are the instability of  $f_{\text{fnc}}$  used for active stabilization of both the 7- and 32-km systems, divided by 2 for a fair comparison against the one-way out-of-loop instabilities. Also shown is a solid black line indicating the effect of 1 radian of accumulated phase noise during the averaging time; the 7-km measurement lies below this level for averaging times  $> 10^3$  seconds. The 7-km fiber transfer (reflection method) is locked continuously for 70 hours, and for frequency counting  $f_{\text{tfr,tfr}}^{(7)}$  with a 10-s gate time, only 0.3% of the counts are outliers. The transfer's accuracy (residual offset from the expected frequency) is  $1 \times 10^{-19}$ , consistent with the long-timescale instability. The 32-km system is continuously locked for several hours at a time for 14 hours (net 85% duty cycle), with a similar amount of outliers. Brief interruptions are caused by the clock laser or the fs frequency comb losing lock, not the transfer or transceiver lasers or the fiber noise cancellation. The accuracy is  $5.2 \times 10^{-19}$ , again consistent with the measured instability from the diurnal temperature fluctuation. To achieve  $10^{-17}$  ( $10^{-19}$ ) accuracy at 1-s ( $10^5$ -s), the various  $\sim 100$ -MHz rf frequency references used for frequency offsets and phase locks must be accurate to  $\sim 3 \times 10^{-11}$  ( $3 \times 10^{-13}$ ).

Both the 7- and 32-km measurements are limited by fluctuations of the out-of-loop optical components used to mix the various optical frequencies. This is confirmed by replacing the 7-km fiber with a 2-m fiber, yielding identical results for timescales up to  $10^4$  s, even though the passive instability of the 2-m fiber is 100 times smaller than for the 7-km fiber. The system is enclosed in a box to isolate the out-of-loop optics from air currents and acoustic pickup; without the box the 1-s instability rises to several parts in  $10^{16}$ . The excess instability at  $2 \times 10^4$  s is caused by daily temperature drift of the laboratory. The 32-km measurement is a factor of 2.5 worse than the 7-km measurement at all averaging times, suggesting that the limitation is still the out-of-loop measurement system with greater instability due to its larger complexity. This fact is consistent with a comparison of the instabilities of the 7-km and 32-km transceiver links (measured by counting  $f_{\text{tfr,rpt}}^{(7)}$  and  $f_{\text{tfr,rpt}}^{(32)}$ , respectively) which are identical for averaging times up to 1000 s.

The fiber transfer's coherence is revealed by a direct measurement of the phase noise it introduces. Figure 4(a) shows the phase-noise spectral density  $S_\phi(f)$  of the 7-km fiber network (upper curve in red), measured by comparing the phase of  $f_{\text{tfr,tfr}}^{(7)}$  against a phase-stable rf reference. The lower curve (in blue) shows the same measurement when the 7-km fiber is replaced by the 2-m fiber. For Fourier frequencies between a few Hz and the 1.3-kHz servo bandwidth, the active noise cancellation of the 7-km fiber does not achieve the measurement noise floor represented by the 2-m data. However, below a few Hz the out-of-loop measurement scheme dominates the noise, and is common to both lengths of fiber. The in-

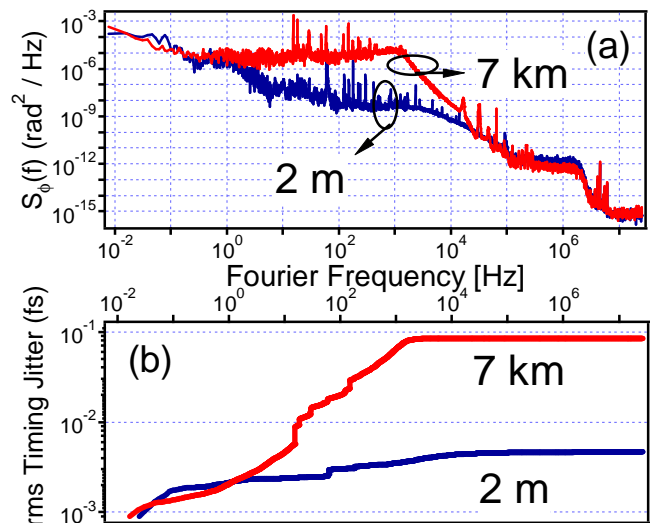


FIG. 4: (color online) (a) Relative phase noise spectral density between the local cw transfer laser and light exiting the 7-km fiber link at the remote end. (b) The relative phase noise shown in (a) is integrated and displayed as rms timing jitter, demonstrating 7-km timing transfer with 0.08 fs of jitter integrated from 8 mHz to 25 MHz.

tegrated phase noise is displayed as rms timing jitter in Fig. 4(b). Integrated from 8 mHz to 25 MHz, only 0.085 fs of timing jitter is accumulated, corresponding to 0.15 rad at the optical transfer frequency of 282 THz.

We acknowledge funding support from ONR, NIST, and NSF. We are grateful to J. Bergquist, T. Schibli, D. Hudson, S. Blatt, M. Boyd, T. Zelevinsky, and G. Campbell for technical help and discussions, and N. Newbury for loan of equipment.

- 
- [1] W. H. Oskay *et al.*, Phys. Rev. Lett. **97**, 020801 (2006).
  - [2] M. M. Boyd *et al.*, Phys. Rev. Lett. **96**, 083002 (2007).
  - [3] S. M. Foreman *et al.*, Rev. Sci. Instr. **78**, 021101 (2007).
  - [4] R. F. C. Vessot *et al.*, Phys. Rev. Lett. **45**, 2081 (1980).
  - [5] J. C. Bergquist *et al.*, in *Frontiers in Laser Spectroscopy, Proceedings of the International School of Physics, "Enrico Fermi:"* Course 120, edited by T. W. Hänsch and M. Inguscio (North-Holland, Amsterdam, 1992), p. 359
  - [6] L.-S. Ma *et al.*, Opt. Lett. **19**, 1777 (1994).
  - [7] F. Narbonneau *et al.*, Rev. Sci. Instr. **77**, 064701 (2006).
  - [8] J. Ye *et al.*, J. Opt. Soc. Am. B **20**, 1459 (2003).
  - [9] G. Grosche *et al.*, CLEO paper CMKK1, 2007.
  - [10] A. D. Ludlow *et al.*, Phys. Rev. Lett. **96**, 033003 (2006).
  - [11] I. Coddington *et al.*, Nature Photonics **1**, 283 (2007).
  - [12] M. Musha *et al.*, Appl. Phys. B **82**, 555 (2006).
  - [13] R. W. Schoenlein *et al.*, Science **274**, 236 (1996).
  - [14] A. L. Cavalieri *et al.*, Phys. Rev. Lett. **94**, 114801 (2005).
  - [15] C. W. Oates *et al.*, Opt. Lett. **25**, 1603 (2000).
  - [16] A. D. Ludlow *et al.*, Opt. Lett. **32**, 641 (2007).
  - [17] S. C. Rashleigh *et al.*, Opt. Lett. **3**, 60 (1978).
  - [18] B. C. Young *et al.*, Phys. Rev. Lett. **82**, 3799 (1999).

[19] T. M. Fortier *et al.*, Opt. Lett. **31**, 1011 (2006).